Metallic phase in the two-dimensional ionic Hubbard model

K. Bouadim,[1] N. Paris,[2] F. Hébert,[1] G. G. Batrouni,[1] and R. T. Scalettar[2]
[1]*INLN, Université de Nice Sophia-Antipolis, CNRS, 1361 route des Lucioles, 06560 Valbonne, France*
[2]*Physics Department, University of California, Davis, California 95616, USA*
(Received 15 May 2007; revised manuscript received 18 June 2007; published 9 August 2007)

We investigate the phases of the ionic Hubbard model in a two-dimensional square lattice using determinant quantum Monte Carlo. At half-filling, when the interaction strength or the staggered potential dominates, we find Mott and band insulators, respectively. When these two energies are of the same order, we find a metallic region. Charge and magnetic structure factors demonstrate the presence of antiferromagnetism only in the Mott region, although the externally imposed density modulation is present everywhere in the phase diagram. Away from half-filling, other insulating phases are found. Kinetic energy correlations do not give clear signals for the existence of a bond-ordered phase.

DOI: 10.1103/PhysRevB.76.085112 PACS number(s): 71.10.Fd, 71.30.+h, 02.70.Uu

I. INTRODUCTION

Tight binding models, such as the Hubbard Hamiltonian, have been widely studied for their ability to describe different kinds of insulating phases present in condensed matter systems. Interactions between fermions give rise to gapped Mott insulators where the fermions are immobile at commensurate fillings. For bipartite lattices, Mott behavior is typically associated with antiferromagnetic order. On the other hand, the imposition of an external periodic potential can drive band insulating behavior. In systems where several types of insulating effects are present, phase transitions can take place as the relative strength of the parameters is changed. Close to such transitions, the competition between these different terms allows smaller effects, such as kinetic energies, to result in low temperature metallic phases or more exotic types of correlations such as bond order. Such compensating effects are believed to explain enhanced response in different quasi-one-dimensional systems such as organic materials,[1] ferroelectric perovskites,[2] or transition metal oxides.[3]

A simple model exhibiting this kind of behavior is the ionic Hubbard Hamiltonian,[4] a tight binding model that includes an on-site repulsion and a staggered potential that takes alternating values on neighboring sites of a bipartite lattice. At half-filling, the on-site repulsion drives the system into an antiferromagnetic Mott insulator (MI), with a homogeneous density. When the staggered potential dominates, a band insulator (BI) with a regular modulation of the density results. A quantum phase transition between these two states occurs in the phase diagram.

In one dimension, the ionic Hubbard model has been widely studied through a variety of techniques including density matrix renormalization group, exact diagonalization, bosonization, and quantum Monte Carlo (QMC) with on-site[5–8] or extended[2,3,9–12] interactions. The precise conclusions are still subject to some debate, but many of the studies suggest that the direct transition from the band insulator to the Mott insulator is replaced by an intervening insulating bond-ordered phase. In two dimensions, cluster dynamical mean field theory[13] (DMFT) and determinant quantum Monte Carlo[14] (DQMC) were used. The existence of an intermediate phase between the BI and MI phases has been established, as in one dimension, but the precise nature of the phase is still under debate (see Sec. II). In infinite dimension,[15,16] similar results are found with DMFT with a low temperature metal as the intermediate phase. Such a metallic phase is also found in a bilayer Hubbard model,[17] where the band structure with a gap is generated by a sufficiently large interplane hopping. A recent experiment attempted to observe this kind of phase.[18,19] Some of the phenomena presented here also have similarities with those found in corresponding disordered models used to describe binary alloys.[20]

In this paper, we consider the different phases and transitions of the ionic Hubbard Hamiltonian on a two-dimensional square lattice using determinant DQMC, extending our initial study.[14] In Sec. II, we introduce the model and summarize our previous results. In Sec. III, we briefly describe the numerical techniques used while in Sec. IV, we investigate further the different phases by measuring the charge and magnetic structure factors and the spectral function. We then present an analysis of the properties away from half-filling (Sec. V) and the search for bond-order waves (Sec. VI). Conclusions are in Sec. VII.

II. FERMIONS IN A STAGGERED POTENTIAL

We consider the ionic Hubbard model

$$\hat{H} = -t \sum_{\langle \mathbf{r}\mathbf{r}'\rangle\sigma} (c^{\dagger}_{\mathbf{r}\sigma} c_{\mathbf{r}'\sigma} + c^{\dagger}_{\mathbf{r}'\sigma} c_{\mathbf{r}\sigma}) + U \sum_{\mathbf{r}} n_{\mathbf{r}\uparrow} n_{\mathbf{r}\downarrow} + \sum_{\mathbf{r}} \left[\frac{\Delta}{2} (-1)^{(x+y)} - \mu \right] (n_{\mathbf{r}\uparrow} + n_{\mathbf{r}\downarrow}), \quad (1)$$

where $c^{\dagger}_{\mathbf{r}\sigma}(c_{\mathbf{r}\sigma})$ are the usual fermion creation (destruction) operators on site $\mathbf{r}=(x,y)$ of a two-dimensional square lattice with spin σ ($\langle \mathbf{r}\mathbf{r}' \rangle$ denotes the pairs of neighboring sites) and where $n_{\mathbf{r}\sigma}=c^{\dagger}_{\mathbf{r}\sigma}c_{\mathbf{r}\sigma}$ is the number operator. The hopping parameter t sets the energy scale and is fixed at a value of 1, while tuning the chemical potential μ gives the desired fermion filling. The interaction strength U and staggered potential $(-1)^{(x+y)}\Delta/2$ are the two competing terms of our system,

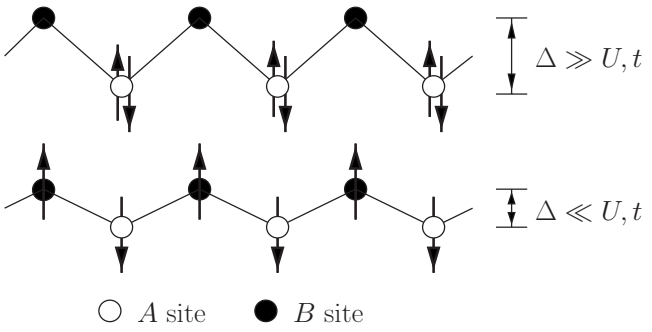

FIG. 1. Schematic diagram of electrons in a staggered potential. The A sites have lower chemical potential than the B sites (the difference being Δ). For low interaction strength $U \ll \Delta$, the electrons prefer to doubly occupy the A sites and form a band insulator. For $U \gg \Delta$, it is favorable to have only one electron per site and to form a Mott insulator. The hopping term t then generates an antiferromagnetic modulation.

the former encouraging single occupancy of all sites and the latter double occupancy of the low energy sublattice.[21] The density ρ is defined as the total number of particles divided by the number of sites in the lattice.

Considering the limiting cases $U \gg \Delta$ and $\Delta \gg U$, we find two distinct insulating phases at half-filling (density $\rho=1$). For $\Delta=0$, the usual translationally invariant Hubbard model arises and, at $T=0$, forms an antiferromagnetic Mott insulator at half-filling for any value of U. At strong coupling, the gap is set by U, while the effective antiferromagnetic coupling is set by $J=4t^2/U$. These two energy scales are evident in the magnetic properties where $T \sim U$ demarks the onset of moment formation on individual sites and $T \sim J$ the onset of antiferromagnetic order between sites.

In the noninteracting limit $U=0$, the Hamiltonian can be diagonalized in Fourier space (where it reduces to a set of independent 2×2 matrices),

$$\hat{H} = \sum_{\mathbf{k},\sigma} E_{\mathbf{k}} c^{\dagger}_{\mathbf{k}\sigma} c_{\mathbf{k}\sigma} \quad \text{with } E_{\mathbf{k}} = \pm \sqrt{\epsilon^2_{\mathbf{k}} + (\Delta/2)^2},$$

where the sum runs over half the Brillouin zone and where $\epsilon_{\mathbf{k}} = -2t(\cos(k_x) + \cos(k_y))$ is the energy of a free particle of wave vector $\mathbf{k}=(k_x,k_y)$. The eigenenergies $E_{\mathbf{k}}$ are then split into two bands separated by a gap Δ and, in this limit, the system is a band insulator at half-filling. These two insulating phases can be seen schematically in Fig. 1.

Recently, it was shown by DMFT[15,16] in infinite dimension and by cluster DMFT[13] and DQMC[14] in two dimensions that there is no direct transition between these two insulating phases, but that an intermediate phase appears (Fig. 2). The infinite and two dimension phase diagrams differ qualitatively. In infinite dimensions, the intermediate phase extends to the $\Delta=0$ line, whereas in two dimensions, the intermediate phase is only present when U and Δ are both nonzero. The phase diagrams obtained by cluster DMFT and DQMC in two dimensions agree quantitatively as far as the boundaries of the intermediate phase are concerned (for example, the intermediate phase is located slightly above the strong coupling boundary and the extents of this phase are similar[21]),

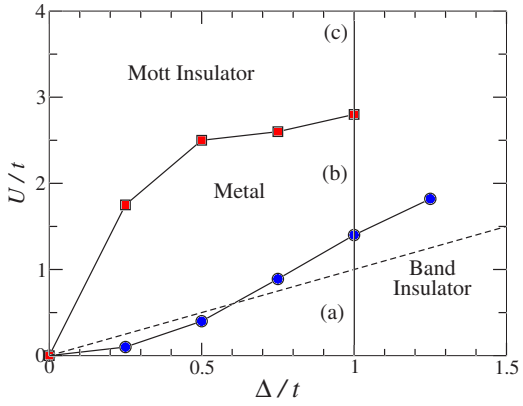

FIG. 2. (Color online) The phase diagram of the ionic Hubbard model (Ref. 21). The symbols are the result of QMC simulations. The dashed line is the strong coupling ($t=0$) phase boundary between band and Mott insulators. Points (a), (b), and (c) located, respectively, in the BI, the intermediate phase, and the MI are used in Fig. 3.

while the precise nature of this phase is still being debated. In infinite dimension, Garg *et al.*[15] and Craco *et al.*[16] found that the intermediate phase is a metal. In a previous work,[14] we used the DQMC algorithm to study the conductivity of the model in two dimensions. Performing a finite size and temperature analysis, we also concluded that the intermediate phase has a finite conductivity and is, consequently, metallic. On the contrary, Kancharla and Dagotto argued for a bond-ordered wave (BOW) phase.[13] DMFT studies[13,16] show the presence of first order transition between the intermediate phase and the Mott insulator. In our DQMC work, we found continuous evolution of the measured quantities when U or Δ are varied, which could suggest a second order transition. However, the limited sizes used in DQMC could also be the reason for this continuous behavior, even in a system experiencing a first order transition in the thermodynamic limit. It is then impossible to establish the nature of the phase transition with the DQMC approach on such limited lattice sizes.

III. COMPUTATIONAL METHODS

DQMC[22] is a numerical approach which expresses the partition function $Z=\mathrm{Tr}\exp(-\beta H)$ as a path integral where the inverse temperature β is discretized. The interaction term is decoupled via a Hubbard-Stratonovich (HS) transformation, introducing a sum over an Ising spin field and leaving the Hamiltonian in a quadratic form with respect to the fermion operators. The fermionic degrees of freedom can then be integrated out and the remaining Boltzmann weight is expressed as the determinant of the product of two matrices that depend on the HS spin variables. In the conventional Hubbard model, this determinant is positive at half-filling due to particle-hole symmetry. With the staggered potential, the determinant is no longer always positive at half-filling, resulting in a sign problem which can be severe.

The remaining sum over the HS field and the evaluation of observables are achieved by a Metropolis Monte Carlo algorithm. It is difficult to obtain good estimates for the ob-

servables when the determinant is often negative, i.e., when the mean value of the sign of the determinant is small. This problem is important for intermediate values of U and Δ, while it is not severe in the limiting cases where we retrieve simple BI or MI phases (U or Δ small or large).

With this formulation, space and (imaginary) time separated Green functions

$$G(\mathbf{R},\tau) = \langle c_{\mathbf{r}+\mathbf{R}\sigma}(\tau) c^{\dagger}_{\mathbf{r}\sigma}(0)\rangle$$

are easily expressed as elements of the matrices. From the spatial Fourier transform of $G(\mathbf{R},\tau)$, one can extract the spectral function (essentially the density of states) by inverting the Laplace transform

$$G(\mathbf{k}=0,\tau) = \int d\omega \frac{e^{-\omega\tau}}{1+e^{-\beta\omega}} A(\omega). \quad (2)$$

Solving for $A(\omega)$ remains a nontrivial task that is performed with a method of analytic continuation.[23] We tested this method in the well-known cases where $\Delta=0$. We measure correlation functions for charge density wave (CDW) and spin density wave (SDW), given by

$$C^{\mathrm{CDW}}_{\mathrm{SDW}}(\mathbf{R}) = \frac{1}{N}\sum_{\mathbf{r}} \langle [n_{\mathbf{r}+\mathbf{R}\uparrow} \pm n_{\mathbf{r}+\mathbf{R}\downarrow}][n_{\mathbf{r}\uparrow} \pm n_{\mathbf{r}\downarrow}]\rangle,$$

where + corresponds to CDW and − to SDW. The staggered potential imposes a checkerboard modulation on the density, not only in the BI phase but in all phases as it breaks explicitly the translational invariance. Antiferromagnetic magnetic correlations are also expected in the MI phase. Thus, for both types of correlations, we expect ordering with a wave vector $\mathbf{k}_{\pi}=(\pi,\pi)$, characterized by the divergence of corresponding structure factors

$$S^{\mathrm{CDW}}_{\mathrm{SDW}} = \sum_{\mathbf{R}} e^{i\mathbf{k}_{\pi}\cdot\mathbf{R}} C^{\mathrm{CDW}}_{\mathrm{SDW}}(\mathbf{R}). \quad (3)$$

IV. SPECTRAL FUNCTION MAGNETIC AND CHARGE ORDERS

To complete our previous analysis[14] of the intermediate phase shown in Fig. 2, we evaluated the charge and spin correlations and spectral function. When the size is not explicitly mentioned, we used an $N=6\times6=36$ site lattice. $N_x=\sqrt{N}$ denotes the side of the lattice.

Figure 3 shows the spectral function for $\Delta=1$ (along the vertical line shown in Fig. 2) at $\beta=12$ and for three values of U corresponding to the three different phases. For $U=0.5$ and $U=4$, corresponding to the BI and MI phases, the spectral function shows a gap around $\omega=0$, thus indicating an insulator. In contrast, the spectral function for $U=2$ is nonzero and shows a quasiparticle peak at $\omega=0$, which indicates metallic behavior. Similar behaviors of the spectral function were found in the different DMFT studies of this system.[13,15,16]

These results are consistent with measurements of the conductivity in our previous article, as is confirmed by the direct comparison of the spectral function at zero frequency

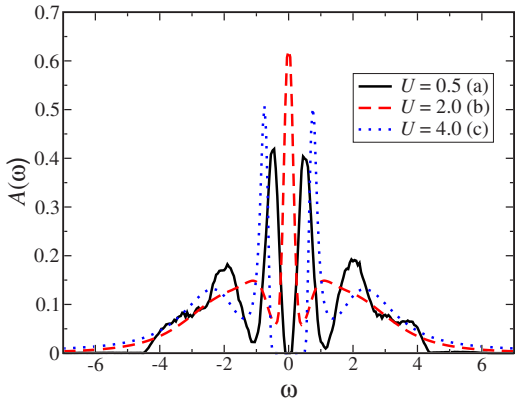

FIG. 3. (Color online) Spectral function $A(\omega)$ for various values of interaction strength U with $\Delta=1$ on a 6×6 lattice at $\beta=12$ at half-filling. The letters (a)–(c) correspond to points on the phase diagram in Fig. 2. Point (b) exhibits a metallic behavior as $A(\omega)$ is nonvanishing for $\omega=0$. $A(\omega)$ exhibits clear gaps for points (a) and (c) which are, respectively, band and Mott insulating states.

$A(\omega=0)$ and the conductivity σ_{dc} shown in Fig. 4. For $\Delta=0.5$ and as U is increased, the behaviors of these two quantities are similar. They both show, for intermediate values of U, a peak that grows with β. The ranges of interaction where there are peaks are slightly different because of finite size effects.

U_{c1} and U_{c2} are the critical repulsion energies that cause BI to metal and metal to MI phase transitions for a fixed value of Δ. These critical values are obtained by a finite temperature analysis of the conductivity.[14] As the temperature is lowered, the conductivity increases in a metal and decreases in an insulator. Locating the points where the behavior of the conductivity changes gives the critical values. For $\Delta=0.5$, the BI-metal transition is located at $U_{c1}/t\simeq0.5$, the metal-MI transition is located at $U_{c2}/t\simeq2.5$, and the metallic region is in between.

Structure factors S_{SDW} and S_{CDW} are shown in Fig. 5 for $\Delta=0.25$ and for inverse temperatures $\beta=10$, 12, and 16. For these values of Δ, the metallic boundaries are $U_{c1}\simeq0.1$ and

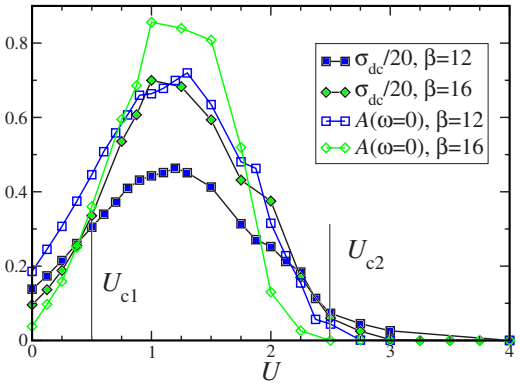

FIG. 4. (Color online) The spectral function $A(\omega)$ and conductivity σ_{dc} are shown as functions of U at $\beta=12$ and 16, at half-filling, and for $\Delta=0.5$. There is a BI-metal transition at $U_{c1}\simeq0.5$ and a metal to MI transition at $U_{c2}\simeq2.5$.

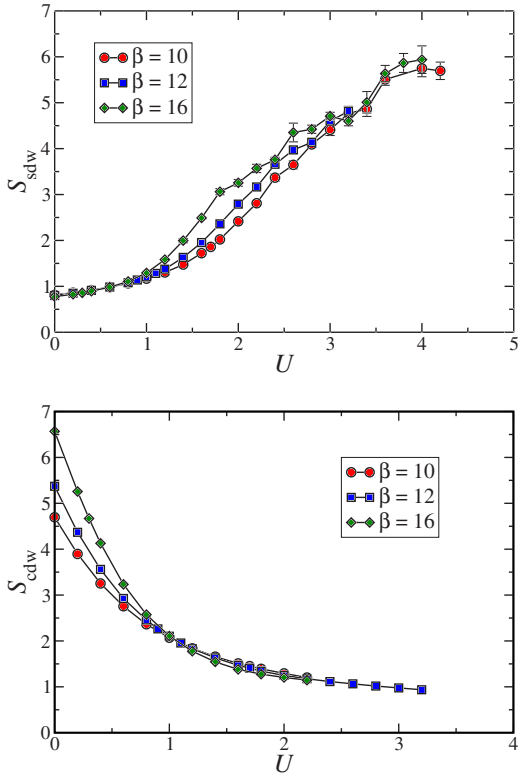

FIG. 5. (Color online) Top: Antiferromagnetic structure factor S_{SDW} as a function of repulsion U showing antiferromagnetic order developing for large U. Bottom: Conversely, the charge structure factor S_{CDW} decreases as U increases. $\Delta=0.25$ in both figures.

$U_{c2} \simeq 1.7$. As U is increased, S_{SDW} increases as the system is driven towards the MI phase, while S_{CDW} decreases in moving away from the BI phase. The transitions in these quantities when we cross the phase boundaries are not sharp on lattices of fixed, finite size owing to finite size rounding effects. In addition, as stated above, a smoother evolution is expected for S_{CDW} as a modulation of ρ is imposed by the external potential for all parameter values.

In a conventional Hubbard model, the MI at half-filling is always an antiferromagnet. However, it has been suggested recently for related models[17] that the metal-MI and paramagnetic to antiferromagnetic (PM-AF) transitions may not take place together. A finite size scaling analysis of S_{SDW} for different values of U is needed to check whether these two boundaries coincide in our model. The structure factor S_{SDW} increases like the number of sites N in the thermodynamic limit

$$\frac{S_{SDW}}{N} = \frac{m^2}{3} + O\left(\frac{1}{N_x}\right), \tag{4}$$

where m^2 is the antiferromagnetic order parameter. Figure 6 shows structure factors for sizes up to $N=12\times12$ sites for different values of U. Δ is set to 0.5 and the metallic phase appears between $U_{c1} \simeq 0.5$ and $U_{c2} \simeq 2.5$. We apply a least-squares fit to the data and extrapolate to an infinite system. We find a nonvanishing structure factor only in the MI phase ($U=2.75$ and 3). In all the other cases, including points located close to the metal-MI transition ($U=2.25$ and 2.5), the structure factor goes to zero as the size is increased.

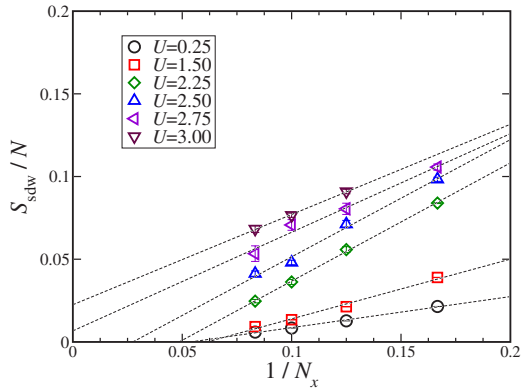

FIG. 6. (Color online) The antiferromagnetic structure factor S_{SDW}/N as a function of inverse lattice size $1/N_x$ at $\Delta=0.5$ and $\beta=12$ for various U. The different values of U correspond to different phases: $U=0.25$ to the BI, $U=1.50, 2.25$ and 2.5 to the metal, and $U=2.75$ and 3 to the MI. The lines are least-squares fit to the data and the extrapolation leads to the value of $S_{SDW}=m^2/3$ for an infinite system. There is antiferromagnetic long range order only in the MI phase.

The PM-AF transition, therefore, takes place between $U=2.5$ and $U=2.75$ and appears to be simultaneous with the metal-MI transition. Although our study on limited sizes cannot completely exclude the possibility of an exotic AF metallic phase located around the metal-MI boundary, our data suggest that it does not occur.

V. AWAY FROM HALF-FILLING

We extend our study to determine the behavior away from the half-filled band. In Fig. 7, the density ρ is plotted as a function of chemical potential. The compressibility κ is given by $\partial\rho/\partial\mu$. For $\kappa=0$, incompressible insulating phases are present, which is indicated by plateaus in the ρ versus μ

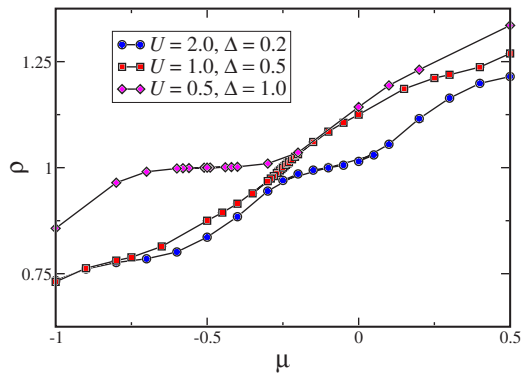

FIG. 7. (Color online) Density ρ as a function of chemical potential μ for the different phases. The Mott ($U=2.0, \Delta=0.2$, circles) and band ($U=0.5, \Delta=1.0$, diamonds) insulating phases have plateaus as the compressibility $\kappa=\partial\rho/\partial\mu=0$ at half-filling. For the metallic phase ($U=1.0, \Delta=0.5$, squares), there is no plateau in the region around $\rho=1$.

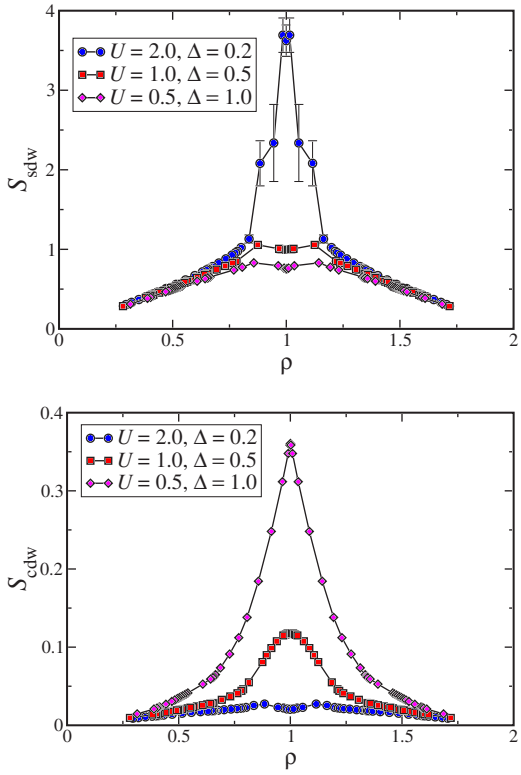

FIG. 8. (Color online) Spin (top) and charge (bottom) structure factors as functions of density. The parameters are the same as in Fig. 7. As ρ approaches half-filling, S_{SDW} reaches its maximum value for the Mott phase. Conversely, S_{CDW} is maximum at $\rho=1$ for the band insulator. The metallic phase has a slight peak in S_{CDW} but not in S_{SDW}.

curve. Both the MI ($U=2.0, \Delta=0.2$) and BI ($U=0.5, \Delta=1.0$) phases have this distinctive plateau at half-filling. The metallic nature of the intermediate phase is once again confirmed by the absence of a plateau around $\rho=1$.

Using the same parameters U and Δ, we show in Fig. 8 the evolution of the structure factors as functions of ρ. As expected, for the parameters corresponding to the MI at $\rho=1$, S_{SDW} shows a strong peak around half-filling indicating the presence of the AF-MI transition in this case and its rapid suppression upon doping. In this case, charge correlations always remain small, as double occupancy of sites is essentially forbidden. Similarly, for the parameters corresponding to the BI, the peak is present in S_{CDW} at $\rho=1$ and S_{SDW} remains small for all densities, as the occupation of the larger energy site is suppressed. For the metallic case, there is no peak in the magnetic structure factor at $\rho=1$ but a moderate peak in S_{CDW}.

In all these three cases, away from half-filling, the structure factors are rapidly suppressed and the system is compressible and becomes a paramagnetic metal.

For stronger interactions and staggered potential, other ordered phases can be found at quarter and three-quarter fillings. For $U=4$ and $\Delta=8$, there is a band insulator at half-filling shown by the $\rho=1$ plateau in Fig. 9. Additional plateaus emerge at $\rho=0.5$ and 1.5. The plateau at $\rho=0.5$ corresponds to a state where all the lower energy sites are

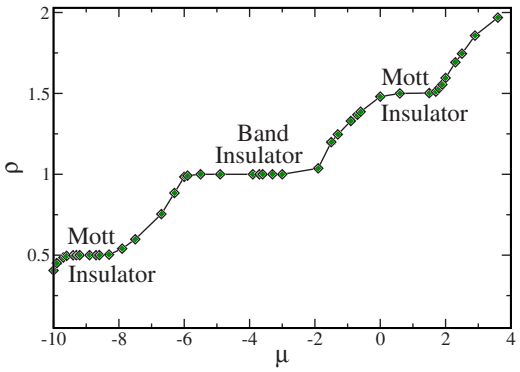

FIG. 9. (Color online) The density ρ as a function of chemical potential μ for $\Delta=8$ and $U=4$ at $\beta=10$. The plateaus represent the various insulating phases. The regions where $\kappa>0$ are metallic phases.

occupied by one fermion. Adding a fermion to an already occupied site increases the energy approximately by U, while adding it to an empty (high energy) site increases it by Δ. There is then an energy gap, roughly equal to the smaller of the two parameters (U in this case). We then have a Mott insulator at quarter filling and, symmetrically, another one at three-quarter filling. In the case where U is larger than Δ, the situation is reversed and we expect a MI at half-filling and a BI for $\rho=0.5$ and $\rho=1.5$ (this case is difficult to treat numerically because of a strong sign problem).

Although the system is incompressible for $\rho=0.5$, there is no concomitant magnetic order. In Fig. 10, S_{SDW} always remains small as ρ is varied away from half-filling and there is no AF peak around quarter filling (the maximum being around $\rho=0.75$). The AF ordering appears when the fermions jump between neighboring sites, thus creating an effective antiferromagnetic coupling between spins. At quarter filling, the particles are surrounded by empty sites and there is no effective coupling. As for S_{CDW}, we only observe a peak at half-filling (Fig. 10). A plot of the conductivity [Fig. 10(c)] versus ρ shows that, indeed, σ_{dc} vanishes for $\rho=1/4$ and $\rho=3/4$ corresponding to the plateaus observed in Fig. 9.

VI. BOND-ORDERED WAVES

Long range BOWs are known to exist in one dimension in the ionic Hubbard model[6–8] as well as in other one-dimensional systems exhibiting density modulation such as extended Hubbard models.[10,11] In the latter case, the two numerical treatments, using the stochastic series expansion[11] and density matrix renormalization group,[10] disagree on the precise width of the BOW phase as well as over what range of coupling values it is present. It was suggested by Kancharla and Dogotto[13] that the intermediate phase observed at half-filling in the two-dimensional case studied here was in fact a bond-ordered state, as in one dimension. Other studies have attempted to observe bond order in two dimensions, for example, in extended Hubbard models.[24] In two dimensions, bond orders have mostly been obtained in Hamiltonians possessing rather special geometries or interactions, e.g., on

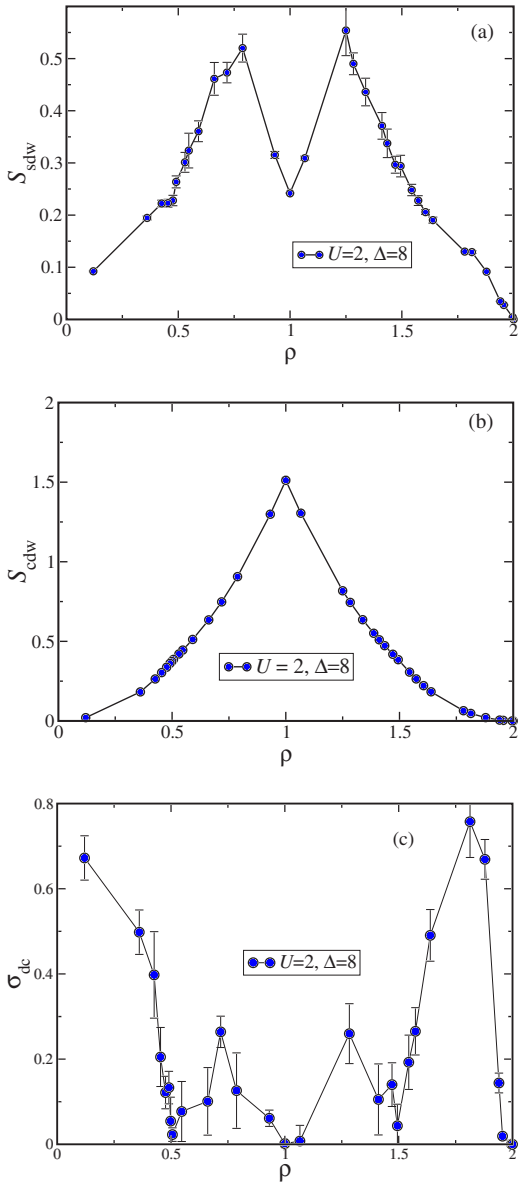

FIG. 10. (Color online) (a) Antiferromagnetic structure factor S_{SDW}, (b) charge structure factor S_{CDW}, and (c) conductivity σ_{dc} as functions of ρ at $U=2$, $\Delta=8$, and $\beta=10$. Note that σ_{dc} vanishes in the three solid phases, $\rho=1/2, 1, 3/2$.

checkerboard lattices[25] or by including additional terms such as ring exchanges.[26]

Hence, bond order seems in general more difficult to obtain in two dimensions than in one. In our system, we can understand this with the argument sketched in Fig. 11. Starting from a situation where all the particles are located on the low energy sites (A sites), a jump to a high energy site (B site) increases the energy roughly by $\Delta-U$. If Δ and U are of the same order of magnitude, this energy cost is small and the jump has a high probability to happen. This B site is connected to two A sites: the one where the jumping particle comes from (to the right in Fig. 11) and another one (to the left) still occupied by two particles. The jumps on the left bond are suppressed. The particle on the B site and the particle having the same spin (an up spin in the sketch) on the A site cannot jump because of Pauli principle, while a jump of the remaining particle has a large energy cost Δ.

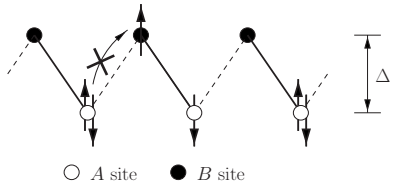

FIG. 11. Schematic diagram of how a bond-ordered wave occurs in one dimension. For $U\sim\Delta$, both large, the electrons may move to a site of higher chemical potential, as shown with the spin-up electron. The spin-down electron in the left well is not likely to move to the right because it will cost a large energy Δ to doubly occupy the site of higher chemical potential. Prohibited movement to the left causes a decrease in kinetic energy for that bond. This alternation of two bonds with weak and strong kinetic energy bonds is an indication of the appearance of a bond order. The continuous thick lines are strong bonds and the dotted lines are weak bonds.

In short, having a particle jumping on a bond (and thus a contribution to the kinetic energy on this bond) will inhibit jumps on the following bond. In one dimension, this can lead to a bond order with alternate strong and weak values of the kinetic energy. On a two-dimensional square lattice, the appearance of a strong bond will inhibit the three other bonds linked to the same site and it seems more difficult to generate regular arrays of weak and strong bonds.

To check if there is a BOW, we examined the correlation function of the kinetic energy,

$$K^{xx}(\mathbf{R}) = \sum_{\mathbf{r}} \langle k^x_{\mathbf{r}+\mathbf{R}} k^x_{\mathbf{r}} \rangle,$$

where $k^x_{\mathbf{r}}$ is the kinetic energy operator connecting sites $\mathbf{r}$ and $\mathbf{r}+\hat{x}$ ($\hat{x}$ being a unit vector directed along the x direction),

$$k^x_{\mathbf{r}} = \sum_{\sigma=\uparrow,\downarrow} (c^\dagger_{\mathbf{r}+\hat{x},\sigma} c_{\mathbf{r},\sigma} + c^\dagger_{\mathbf{r},\sigma} c_{\mathbf{r}+\hat{x},\sigma}).$$

The Fourier transform of $K^{xx}(\mathbf{R})$ always exhibits a very small peak for $\mathbf{k}_\pi=(\pi,\pi)$ in all the different phases at or away from half-filling. Finite size scaling analysis indicates that these peaks persist in large size lattices, but this is the case for all the different phases, not only in the intermediate phase. We also studied the BOW susceptibility[11] for this wave vector,

$$\chi_{\mathrm{BOW}} = \sum_{\mathbf{R},\mathbf{r},\tau} e^{i\mathbf{k}_\pi\cdot\mathbf{R}} \langle k^x_{\mathbf{r}+\mathbf{R}}(\tau) k^x_{\mathbf{r}}(0) \rangle. \quad (5)$$

Figure 12 shows the evolution of χ_{BOW} at half-filling as a function of U and for two different values of Δ. The curve is maximum in the intermediate phase but is also nonzero in other phases. Similar results are obtained for bonds oriented along the y direction and for mixed $x-y$ cases.

We do not believe these signals to indicate the presence of a BOW phase for the following reasons: (a) The values obtained are extremely small. (b) These "BOW signals" are ubiquitous in *all three phases* and not specific to the intermediate one. The susceptibility is, for example, nearly as

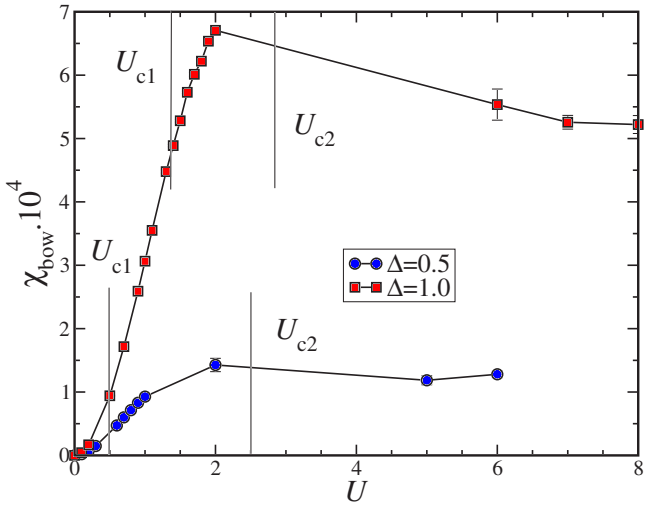

FIG. 12. (Color online) The bond-ordered susceptibility as a function of U at $\rho=1$ for $N=12\times12$ and $\beta=10$. The vertical lines separate the three different phases for two different values of the staggered potential. The maximum of this bond-order parameter is in the metallic region but is of order 10^{-4}.

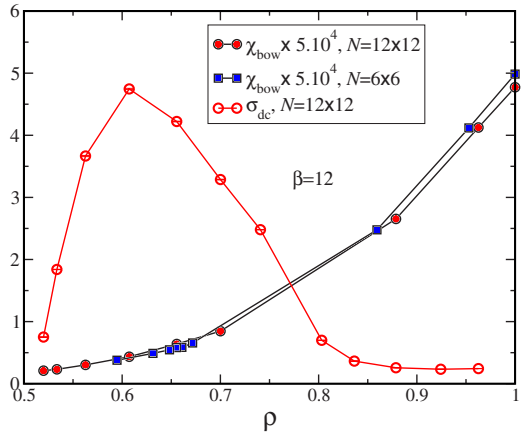

FIG. 13. (Color online) The bond-ordered susceptibility and conductivity as functions of ρ for $\Delta=1$, $U=0.5$, and $\beta=12$. Doping away from half-filling, the susceptibility is nonzero even when the band is only partially full and the system is unquestionably metallic.

important in the MI phase as in the intermediate phase. As soon as U and Δ are both nonzero, we observe this very weak nonzero value of χ_{BOW}. (c) Starting from the metallic phase $(U=0.5,\Delta=1)$ and doping away from half-filling, the system is certainly known to be metallic (see Fig. 13), yet the BOW susceptibility is nonzero and comparable to the value found at half-filling. For all these reasons, we believe that these tiny signals are only a weak signature of an interplay between the interaction and externally imposed checkerboard potential.

VII. CONCLUSIONS

We have extended our previous study of the phase diagram of the ionic Hubbard model.[14] In addition to the QMC results for the conductivity, we calculated the spectral function, the kinetic energy correlation function (the order parameter for the BOW phase), and the magnetic and charge order parameters. Our results point to the presence of a normal conducting metallic phase intervening between the band and Mott insulating phases. In particular, we have not found a clear signal in the BOW order parameter and susceptibilities indicating the presence of such a phase.

We also studied the system doped away from half-filling. When the band or Mott insulating phase is doped, a conducting phase is obtained except at fillings of 1/4 and 3/4, where we found insulating phases without magnetic order.

ACKNOWLEDGMENTS

G.G.B., F.H., and K.B. are supported by a grant from the CNRS (France) PICS 18796. R.T.S. and N.P. are supported by NSF ITR 0313390. The authors acknowledge helpful discussions with M. M. Gibbard.

[1] N. Nagaosa and J. Takimoto, J. Phys. Soc. Jpn. **55**, 2735 (1986); **55**, 2745 (1986); **55**, 2745 (1986) and references therein.
[2] T. Egami, S. Ishihara, and M. Tachiki, Science **261**, 130 (1994).
[3] S. Ishihara, T. Egami, and M. Tachiki, Phys. Rev. B **49**, 8944 (1994).
[4] J. Hubbard and J. B. Torrance, Phys. Rev. Lett. **47**, 1750 (1981).
[5] T. Wilkens and R. M. Martin, Phys. Rev. B **63**, 235108 (2001); M. E. Torio, A. A. Aligia, and H. A. Ceccatto, *ibid.* **64**, 121105(R) (2001); C. D. Batista and A. A. Aligia, Phys. Rev. Lett. **92**, 246405 (2004); G. I. Japaridze, R. Hayn, P. Lombardo, and E. Müller-Hartmann, arXiv:cond-mat/0611415 (unpublished).
[6] A. P. Kampf, M. Sekania, G. I. Japaridze, and Ph. Brune, J. Phys.: Condens. Matter **15**, 5895 (2003).
[7] Y. Z. Zhang, C. Q. Wu, and H. Q. Lin, Phys. Rev. B **67**, 205109 (2003).
[8] S. R. Manmana, V. Meden, R. M. Noack, and K. Schönhammer, Phys. Rev. B **70**, 155115 (2004).
[9] A. A. Aligia and C. D. Batista, Phys. Rev. B **71**, 125110 (2005).
[10] E. Jeckelmann, Phys. Rev. Lett. **89**, 236401 (2002).
[11] P. Sengupta, A. W. Sandvik, and D. K. Campbell, Phys. Rev. B **65**, 155113 (2002).
[12] H. Craig, C. N. Varney, W. E. Pickett, and R. T. Scalettar (unpublished).
[13] S. S. Kancharla and E. Dagotto, Phys. Rev. Lett. **98**, 016402 (2007).
[14] N. Paris, K. Bouadim, F. Hebert, G. G. Batrouni, and R. T. Scalettar, Phys. Rev. Lett. **98**, 046403 (2007).
[15] A. Garg, H. R. Krishnamurthy, and M. Randeria, Phys. Rev. Lett. **97**, 046403 (2006).
[16] L. Craco, P. Lombardo, R. Hayn, G. I. Japaridze, and E. Müller-Hartmann, arXiv:cond-mat/0703814 (unpublished).
[17] S. S. Kancharla and S. Okamoto, Phys. Rev. B **75**, 193103 (2007).

[18] K. Maitim, R. Shankar Singh, and V. R. R. Medicherla, arXiv:cond-mat/0704.0327 (unpublished).
[19] S. S. Kancharla and E. Dagotto, Phys. Rev. B **74**, 195427 (2006); S. Okamoto and A. J. Millis, *ibid.* **70**, 075101 (2004).
[20] K. Byczuk, W. Hofstetter, and D. Vollhardt, Phys. Rev. B **69**, 045112 (2004); P. Lombardo, R. Hayn, and G. I. Japaridze, *ibid.* **74**, 085116 (2006); N. Paris, A. Baldwin, and R. T. Scalettar, *ibid.* **75**, 165113 (2007).
[21] Our previous article (Ref. 14) contained a factor of 2 error in the value of the staggered potential Δ. The correct definition of the Hamiltonian is the one given here. The BI-MI transition line in the $t=0$ limit in Fig. 2 has been modified accordingly.
[22] S. R. White, D. J. Scalapino, R. L. Sugar, E. Y. Loh, J. E. Gubernatis, and R. T. Scalettar, Phys. Rev. B **40**, 506 (1989).
[23] A. W. Sandvik, Phys. Rev. B **57**, 10287 (1998).
[24] M. Murakami, J. Phys. Soc. Jpn. **69**, 1113 (2000).
[25] M. Indergand, C. Honerkamp, A. Laüchli, D. Poilblanc, and M. Sigrist, Phys. Rev. B **75**, 045105 (2007).
[26] R. G. Melko, A. W. Sandvik, and D. J. Scalapino, Phys. Rev. B **69**, 100408(R) (2004).